VERTICAL APPEARANCE OF NEW ENGLAND THUNDERSTORMS ON 3-CM RADAR

by
DAVID LINUS BAILEY

B.A., Fresno State College
(1952)
B.S., Pennsylvania State University
(1954)

SUBMITTED IN PARTIAL FULFILLMENT
OF THE REQUIREMENTS FOR THE
DEGREE OF MASTER OF SCIENCE
at the
MASSACHUSETTS INSTITUTE OF TECHNOLOGY
May 1962

Signature of Author . . . . . .
Department of Meteorology, May 1962

Certified by . . . . . .
Thesis Supervisor

Accepted by . . . . . .
Chairman, Departmental Committee on Graduate Students

Vertical Appearance of New England Thunderstorms

on 3-cm Radar

by
David L. Bailey

Submitted to the Department of Meteorology
on 19 May 1962
in partial fulfillment of the requirements
for the degree of Master of Science

ABSTRACT

The first section of this thesis considers the effects of attenuation on 3-cm radiation. Attenuation amounts were obtained by comparing indicated reflectivities with those measured by a 10-cm band radar which does not suffer from rain attenuation. Observed attenuation compares favorably with values computed from empirical formulae. The effects of attenuation are not limited to the reduction of reflectivity measurements but also cause serious echo distortion by displacing the apparent core of the storm to the near side of the echo region. Asymmetry of the heavy rain area through which the radar beam must pass to reach the storm's core may cause the radar to display the wrong portion of the echo complex as "most intense".

The second portion of the thesis is devoted to a qualitative study of the vertical structure of thunderstorms from range-height indicator (RHI) photographs from the AN/CPS-9 radar. Features such as height, appearance of edges and tops, tilts, number of interior cells, presence of an anvil

top, and elevated reflectivity cores are studied in relation to the intensity and stage of development of the storm.

Typical storms grow and intensify rapidly after initial radar detection. On the RHI they display uniform width and clear, sharp features. Frequently the tops consist of one or more turrets or spires. The length of the mature or active stage varies from 20-30 minutes for single celled storms to several hours for large intense multicelled storms. During this period the internal structure is complex and quite variable. It is found that the number of interior cells tends to be inversely proportional to the relative intensity of the storm. No other consistent behavior pattern could be detected particularly one that will give a clue as to when the storm will dissipate. The storms dissipate rapidly and display fuzzy features on the RHI.

Anvil tops are observed sporatically during the mature and dissipating stages and should not be construed as an indication of a dissipating storm. Tilts contrary to the prevailing synoptic shear are noted for some storms and in two cases are connected with the initial intensification of new storm cells. Dissipating storms tend to tilt in the direction of the prevailing wind shear.

Elevated reflectivity cores are not a frequently observed feature of severe thunderstorms when viewed on the RHI. Distortion and attenuation caused by heavy rain associated with intense storms complicate the interpretation of such feature to the point that it is virtually meaningless.

Thesis Supervisor: Reginald E. Newell
Title: Assistant Professor of Meteorology

ACKNOWLEDGEMENTS

The graduate work for which this thesis is a partial requirement was performed while the author was assigned by the Air Force Institute of Technology for graduate training at The Massachusetts Institute of Technology.

The author wishes to express his appreciation to Dr. Pauline Austin and Professor Reginald Newell for their encouragement and guidance and to the M.I.T. Weather Radar Project for use of the facilities and equipment.

TABLE OF CONTENTS

LIST OF FIGURES

LIST OF TABLES

I. INTRODUCTION

This investigation is concerned with the study of the vertical features of convective storms such as maximum heights, cap or anvil clouds, tilt, variation of radar reflectivity, sharpness of intensity gradients, and internal structure. These features have been studied from photographs of thunderstorms taken on the range-height indicator (RHI) of a 3-cm wavelength radar (AN/CPS-9). The study is a continuation of an earlier pilot study in which an attempt was made to relate the more salient vertical features of convective cells or thunderstorms to particular phases of the storm's existence. The pilot study was prepared from relatively scanty data and it was immediately obvious that RHI pictures should be taken at frequent intervals throughout the storm's life. To meet this requirement, over 2,000 RHI pictures were taken during the summer of 1961.

The terms "convective cell" or "convective storm" can be used to represent at least four separate classes of motion. The first is the very small convective or turbulence cell of the order of 10 meters in horizontal and vertical dimensions. The second class is one or two orders of magnitude larger in the horizontal and perhaps two or three orders larger in the vertical dimension, that is, 100-1,000 meters by

1,000-10,000 meters. It is this class of motion which is usually referred to as a "convective cell". A closely packed group of "convective cells", commonly designated a "convective storm" or "thunderstorm", makes up the third group. It is possible to have storms of this general size which do not produce thunder and lightning, tropical showers and cumulus congestus, for instance. The fourth class is the loose grouping together of thunderstorms to form squall lines or areas. Each class of convective echoes has rather distinct characteristics of growth, motion, character and duration.

Studies of thunderstorms and "convective cells" made by Byers and Braham (1949), Battan (1959), and many others have set forth general statements concerning the motion, intensity and vertical extent of such storms. Byers and Braham worked with data collected by the Thunderstorm Project in 1945-47. The radar data were simple photographs of the plan-position indicator (PPI) and RHI presentations. No gain reduction devices were used, therefore, it was not possible to comment upon the relative intensity of each storm. They found that a thunderstorm has a life expectancy of 1-3 hours, extends vertically to the tropopause or higher, and moves in the general direction of the prevailing upper air winds at 10-20,000 ft. Large thunderstorms are made up of a number of smaller cells. Battan studied the individual cells more closely and found that they have an expected life of 20-60 minutes unless they combine with

other cells.

This study deals mainly with the third classification, or thunderstorm, as mentioned above, and will consider in detail the vertical features of the storms from inception to demise. A close distinction between the scales of motion is made here because rather striking differences of size, duration, and intensity separate the groups. Of necessity some attention must be given to the larger and smaller scale features also.

II. DATA

The data for this study were collected on the two radars operated by the M.I.T. Weather Radar Project. The SCR-615-B (10-cm wave length) was operated on continuous search. Its returning signal was fed into an iso-echo contouring unit which produced a series of averaged, range-corrected contours at selected intensity levels (Kodaira, 1959). When the radar reflectivity (Z, in mm^6/m^3) is converted to rainfall rate (R, in mm/hr) by the empirical relation $Z = 200R^{1.6}$ the contours represent lines of equal rainfall intensity ranging from 2 to over 500 mm/hr. The contour levels are separated by approximately 5 db which corresponds to a factor of 2 in rainfall rate. Geotis (1961) has found that in New England reflectivities greater than that corresponding to a rainfall rate of 100 mm/hr are indicative of hail. Hence at these high reflectivities the empirical relation for R quoted above is no longer a valid indicator of the volume of water being precipitated.

The SCR-615-B is normally operated at 1° elevation angle with occasional scans being made at higher angles to obtain vertical samples. All data are automatically recorded on 35 mm movie film. The contour data were used to identify and track individual storms or cells, provide an accurate measure of the intensity of the echoes, and as a basis

for determining the amount of attenuation present at 3-cm wave lengths.

The AN/CPS-9 (3-cm wave length) was used exclusively for taking RHI photographs. It is equipped with a 10-position step-gain switch which permits the signal intensity to be reduced in discrete increments. The amount of reduction varies somewhat between steps being 5 db per step for gains 4 through 10 (gain 10 is the most sensitive position), and 8-10 db per step for gains 0-3. The threshold for gain 0 is not very stable and cannot be reliably measured. The RHI photographic record serves as the basic data for studying the vertical features of the storms.

On days when thunderstorm activity was expected the radars would be watched closely for the initial echo appearances. As is frequently the case, the strongest activity occurred on holidays or weekends and on these days observations were not begun until well after the storms had formed. A notable exception was 30 June 1961. The data obtained on this day was excellent.

The normal procedure for taking RHI photographs was to scan the PPI for the appearance of a new echo, center the radar beam on the echo, and take RHI pictures. A sequence of pictures was taken beginning with gain 10 then reducing the gain by steps of two until the echo disappeared. A diligent operator can take pictures at the rate of two to three frames per minute. The position of each echo was marked on the PPI to facilitate tracking and sets of RHI photographs were taken at about ten-minute

intervals. During the early stages of development storms could be easily tracked, but as the activity increased and changes in range were necessary it became increasingly more difficult to track several storms. When storms became very large or were at close ranges RHI pictures were taken at several azimuth settings and an attempt was made to find the most intense portion of the storm in azimuth and height.

A curious, but somewhat expected, phenomenon occurred when large intense storms were viewed at close ranges. The operator of the SCR-615-B would give the position of the most intense cell recorded at the 10-cm wave length, and invariably it would fail to coincide with the most intense spot on the PPI of the AN/CPS-9. More will be said about this later.

RHI photographs were taken on many days throughout the summer. On a few days only spotty shower activity was detected and the echo tops remained well below 25,000 ft. These days along with some others for which the data were incomplete were not studied in detail. When the final screening of both RHI and contour data was finished relatively complete data were available for the storms of 30 June, 2, 3, 10, 21 July 1961. Of these dates only the data for 30 June and 10 July are treated in detail.

III. EFFECTS OF ATTENUATION ON 3-cm RADIATION

For moderate to heavy rainfall rates (less than 100 mm/hr) the effect of attenuation on 10-cm radiation can be neglected. This is definitely not true in the 3-cm band. The attenuation studies of Ryde (1945) and the summary of attenuation studies prepared by Gunn and East (1954) give theoretical expressions for the rate of attenuation by rain in the 3-cm band. Ryde's data are listed in tabular form while Gunn and East present an analytic expression. Figure 1 is a graphical comparison of their results. For rainfall rates of 100 mm/hr or less the differences are insignificant. It has been recognized for many years that presentations on 3-cm band radars are severely affected by attenuation. In order to assess the extent of distortions by attenuation some computations have been made of the expected and observed distortions in a thunderstorm.

Since the 10-cm contour data are basically immune to attenuation they depict the actual areal coverage and intensity of precipitation. Vertical profiles of storms can be synthesized from sets of contours taken at several elevation angles and reduced to equivalent 3-cm values by applying the effects of attenuation. The result can be compared with observed RHI photographs. This procedure is simple in principle but in

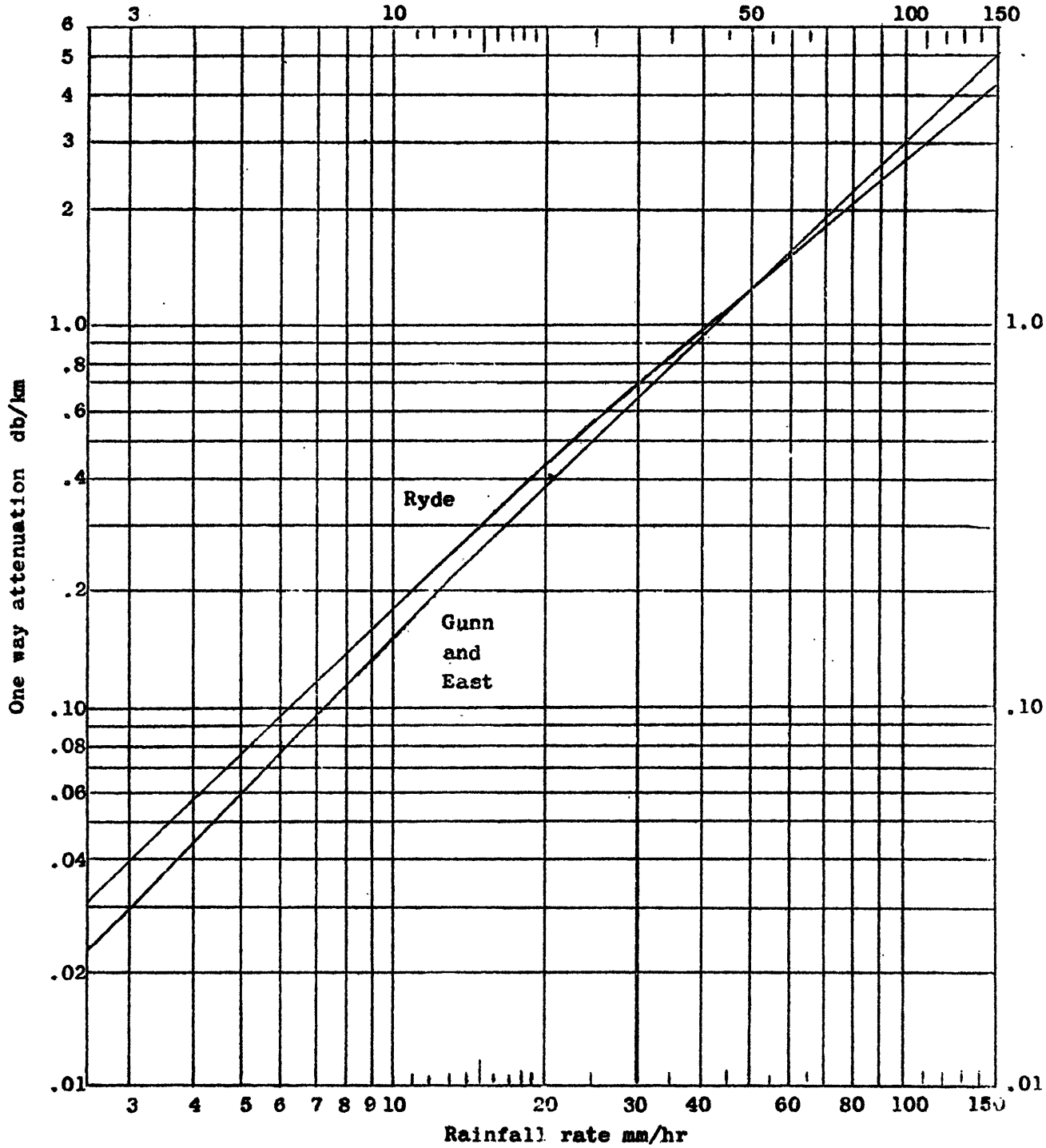

Figure 1. One way attenuation (db/km) as a function of rainfall rate (mm/hr).

practice it is complicated by a number of circumstances. A brief description of the process follows.

The SCR-615-B radar and contouring circuit are closely monitored and calibrated (Austin and Geotis, 1960) so that the observed data are accurate to about 2-3 db. The problems with the contour data are not ones of accuracy but of time and resolution. It takes two minutes or more to complete a cycle of contours at a particular elevation and observations are needed at three to five elevation angles to prepare an acceptable vertical profile. Even if scans are taken as quickly as possible a time lapse of at least 6-10 minutes ensues between the first and last scans. Major changes in the interior structure of thunderstorms can and do occur in this short length of time. The beam width of the SCR-615-B is three degrees and adequate resolution is possible only if the storms are observed within 50 miles of the set. Beyond this range beam filling and smoothing effects are too large to neglect. For these reasons it is necessary to find a storm within the limited range noted which is not experiencing rapid internal changes and for which elevated contour scans and RHI photographs are available.

Unfortunately, the AN/CPS-9 radar is not calibrated as frequently nor as accurately as the SCR-615-B. The gain settings are calibrated only a few times a year and the magnetron spectrum fluctuates appreciably over a period of a few days. It is estimated that these effects reduce

the accuracy of the reflectivity measurements to ± 5-7 db.

The radar equation expresses the power received as a function of the fixed parameters of the radar such as beam width, antenna gain, pulse length, and wave length, and the variable parameters of transmitted power, range, and reflectivity. As noted earlier the reflectivity and rainfall rate are empirically related so that the rainfall rate can be calculated as a function of range and return signal intensity. Table 1 contains the computed values of the rainfall rate R in mm/hr as a function of range in miles and power received in decibels below a milliwatt (-dbm) for the AN/CPS-9 for both long and short pulse modes. The fixed parameters used are: power transmitted, 250 Kw; antenna gain, 41.6 db; beam width, 0.8°; pulse length, 150 meters (short), 600 meters (long); wave length, 3.2 cm. Beam filling effects and variability of transmitted power have been neglected. Values of R greater than 100 mm/hr have little meaning except as indicators of hail. The AN/CPS-9 was calibrated with a signal generator to determine the minimum detectable signal, in dbm, for each gain setting for both long and short pulse. Table 2 gives the average of two calibration techniques. With the aid of Tables 1 and 2 it is possible to determine a rough estimate of the observed reflectivity or rainfall rate at any point. No allowance is made here for differences in threshold between the radar display and the photographic film. The film is somewhat less sensitive so the

Table 1. Computed rainfall rates (R) in mm/hr as a function of range in miles and power received (Pr) in decibels below a milliwatt (-dbm) for both long pulse (LP) and short pulse (SP) positions.

		Range							
Pr	SP	10	20	30	40	50			
-dbm	LP	20	40	60	80	100	125	165	200
94		.05	.11	.20	.27	.36	.47	.63	.84
92		.06	.15	.27	.36	.47	.63	.84	1.1
90		.08	.20	.36	.47	.63	.84	1.1	1.5
88		.11	.27	.47	.63	.84	1.1	1.5	2.0
86		.15	.36	.63	.84	1.1	1.5	2.0	2.7
84		.20	.47	.84	1.1	1.5	2.0	2.7	3.6
82		.27	.63	1.1	1.5	2.0	2.7	3.6	4.7
80		.36	.84	1.5	2.0	2.7	3.6	4.7	6.3
78		.47	1.1	2.0	2.7	3.6	4.7	6.3	8.4
76		.63	1.5	2.7	3.6	4.7	6.3	8.4	11.
74		.84	2.0	3.6	4.7	6.3	8.4	11.	15.
72		1.1	2.7	4.7	6.3	8.4	11.	15.	20.
70		1.5	3.6	6.3	8.4	11.	15.	20.	27.
68		2.0	4.7	8.4	11.	15.	20.	27.	36.
66		2.7	6.3	11.	15.	20.	27.	36.	47.
64		3.6	8.4	15.	20.	27.	36.	47.	63.
62		4.7	11.	20.	27.	36.	47.	63.	84.
60		6.3	15.	27.	36.	47.	63.	84.	110
58		8.4	20.	36.	47.	63.	84.	110	150
56		11.	27.	47.	63.	84.	110	150	200
54		15.	36.	63.	84.	110	150	200	270
52		20.	47.	84.	110	150	200	270	360
50		27.	63.	110	150	200	270	360	470
48		36.	84.	150	200	270	360	470	630
46		47.	110	200	270	360	470	630	840
44		63.	150	270	360	470	630	840	1100
42		84.	200	360	470	630	840	1100	1500
40		110	270	470	630	840	1100	1500	2000

reflectivities will always be underestimated.

Table 2. Minimum detectable signal for each gain setting for long and short pulse modes.

Gain Setting	10	9	8	7	6	5	4	3	2	1
Long Pulse (-dbm)	89	83	77	73	69	65	59	52	44	—
Short Pulse (-dbm)	93	87	81	78	74	70	66	60	61	42

A careful search of all the available contour and RHI data failed to produce a storm which fulfilled all the requirements previously mentioned. By relaxing the restrictions somewhat sufficient data were obtained to permit an analysis of the lower portion of a storm which was observed on 2 July. The storm was part of an intense squall line which passed through eastern Massachusetts during the evening. Contour scans were taken at elevation angles of 1, 3, and 5 degrees.

Figure 3a shows the contour patterns and the unattenuated vertical profile prepared from them. The intensities in Figure 3a are reduced by computed attenuation effects for 3-cm radiation and the results are shown in Figure 3b, labelled in gain setting thresholds for the AN/CPS-9, and Figure 3c, labelled in mm/hr. Figure 3d is a tracing of observed RHI photographs taken at the same time as the contour data. The maximum intensity of the cell at 28 miles as indicated by the AN/CPS-9 is only one-half of that actually occurring. It is reasonable to assume that this cell would

still be seen at gain step 3 which at this range has a threshold in R of about 30 mm/hr. Thus the apparent discrepancy between Figures 3b ar 3c and the RHI photograph vanishes. The remaining cells at about 35 miles are attenuated even more severely. The RHI shows them at less than one fourth of their actual intensity.

In order to show the effects of attenuation on 3-cm radiation more emphatically, the highly idealized thunderstorm shown in Figure 2, which is typical of a strong summertime thunderstorm without hail, was considered. Figure 2b shows the effect of attenuation to 3-cm band values. Only 2-1/2 miles of heavy rain reduces the intensity of the core to less than half of its real value. Note also the apparent displacement of the attenuated core. The total two-way attenuation through the model storm is 23 db which is a factor of more than 20 in rainfall rate. The effects of snow above the melting level has not been considered because in a storm such as this rain drops will be the predominant reflector and attenuator to a height of about 25,000 ft. This assumption is consistent with aircraft observations of rain in varying amounts to heights of 25,000 ft compiled by the Thunderstorm Project. The reflectivity and attenuation properties of the mixture of snow, rain and dry or wet small hail observed at these and higher levels has not been fully explained. For these reasons the rainfall rate attributed to the upper portion of the storm is only tentatively indicated by dashed lines.

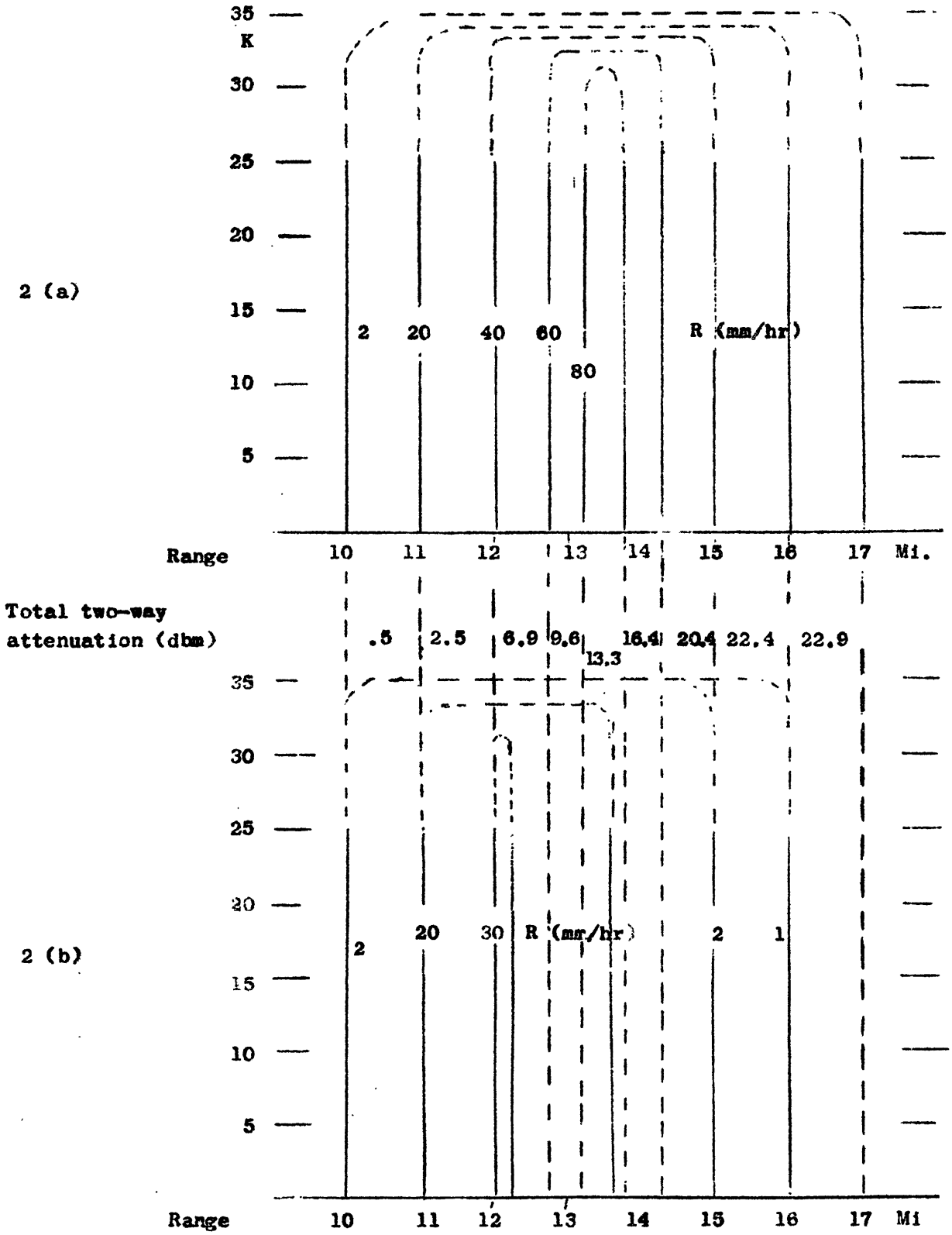

Figure 2. Distortion and attenuation of a model thunderstorm (a) when viewed on the RHI of a 3-cm wave length radar (b).

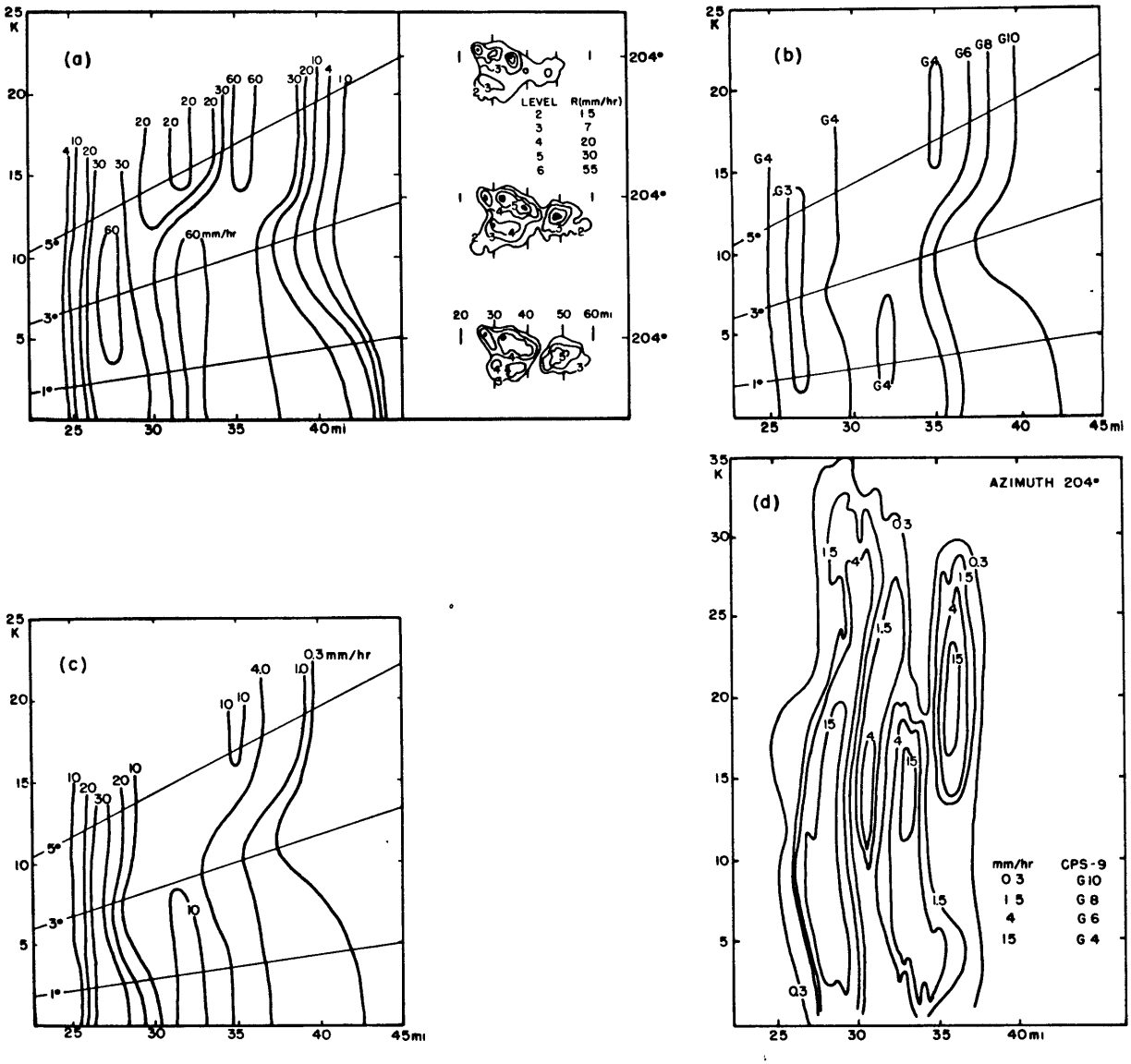

(a) Vertical cross section from 10 cm contour data

(b) and (c) 10 cm. vertical cross sections attenuated to equivalent 3 cm. values

(d) Actual 3 cm. vertical cross section (CPS-9 RHI photos)

Fig. 3. Vertical structure of a convective shower as seen at two wavelengths. Observations made on 2 July 1961, 2155 EST.

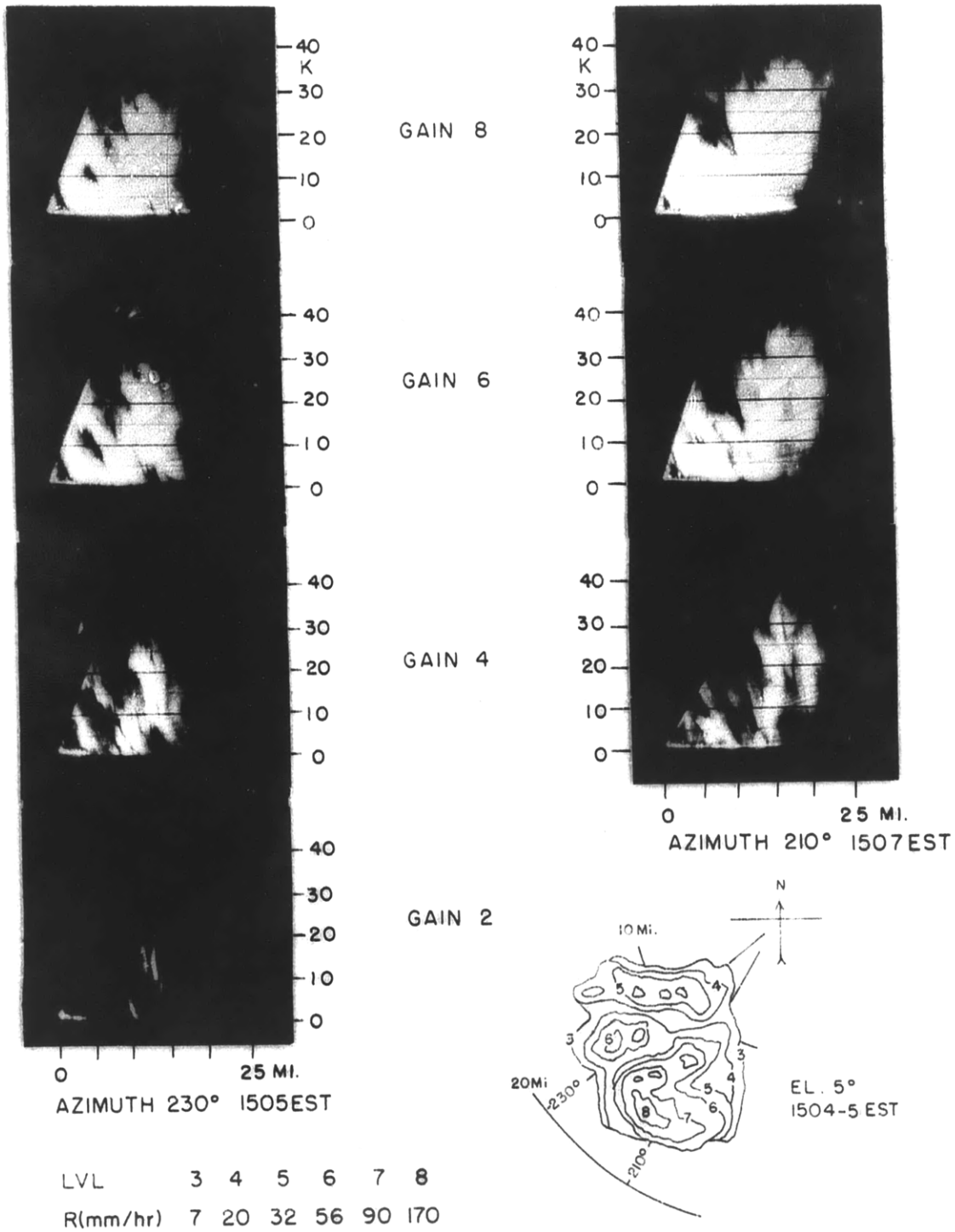

LVL	3	4	5	6	7	8
R(mm/hr)	7	20	32	56	90	170

Fig. 4. Radar data of a severe thunderstorm on 30 June 1961. RHI photographs taken on 3-cm band AN/CPS-9. Contour data is from the 10-cm band SCR-615-B.

The unavoidable conclusion of these simple analyses is that quantitative measurements of radar reflectivities in the vicinity of strong convective storms should not be attempted with 3-cm band radars. Also, any scheme which proposes to identify or analyze severe weather or strong thunderstorm activity with 3-cm radiation is doomed to utter failure. Only when the intense portion of the storm is on the side nearest the radar, and no significant rain intervenes, is it even remotely possible for 3-cm radars to give a representative measurement of the storm's core intensity. Austin (1961) shows examples of nearly simultaneous observations of a squall line by 3-cm and 10-cm band radars. Because of attenuation the 3-cm band radar displays a very poor picture of the position and intensity of the most important cells. Similar reasoning is sufficient to explain why 3-cm and 10-cm band radars do not agree on which portion of an intense storm is the strongest. Figure 4 exhibits an excellent example. The contour pattern from the 10-cm band radar shows a large intense storm with 3 distinct centers of action. The AN/CPS-9 beam at 210° must pass through 6-8 miles of heavy rain before reaching the intense core and the result is severe attenuation. The RHI photographs at this azimuth reflect this effect for the storm was not detected at gain setting 2 (R ~ 45 mm/hr). In contrast, the RHI series at 230°, which has less intervening rain, indicates rainfall rate well in excess of 45 mm/hr for a weaker cell at

the same range. The reflectivity measurement of the intense cell at 210° as shown by the AN/CPS-9 is reduced to 1/4 of its actual value while the weaker cell at 230° has suffered little from attenuation.

Losses suffered through attenuation can be compensated for to a very limited extent. Practical attempts to replace attenuation losses over large areas have been only partially effective. Wein, 1961, describes an electronic system which compensates for attenuation, but it is highly susceptible to calibration errors. No system will be able to reconstruct echoes which have been reduced to the noise level by attenuation.

Effects of attenuation definitely eliminate quantitative measurements of intense thunderstorms by 3-cm band radars; however, much qualitative information can be gleaned from such observations. The next section will deal with the qualitative observation of thunderstorms made from the RHI of a 3-cm band radar.

IV. VERTICAL STRUCTURE OF CONVECTIVE STORMS

A. Models

The data collected by the "Thunderstorm Project" in 1945-47 enabled Byers and Braham (1949) to construct the first model of a thunderstorm which was consistent with combined surface, upper air and radar observations. They found it necessary to divide the storm's life into three distinct phases, each of which is characterized by a particular field of vertical motions. The first or "cumulus stage" begins with the initial convective bubble and continues until precipitation begins. During this period essentially all vertical motions are upward. With the onset of precipitation the storm enters its "mature stage", see fig. 5b, and both positive and negative vertical velocities are present. Vertical motions may reach 30-50 m/sec in either direction during this phase. Precipitation is usually rain at the surface but at higher levels mixtures of rain, snow and hail are encountered. According to Byers and Braham falling precipitation impedes the upward motion of moist unstable air and thus acts to hinder any further development or intensification of the storm. Simultaneously the cold downdraft spreads out under the storm's base and reduces the region from which unstable air can be drawn. At this point the cell enters the final or "dissipating stage", see fig. 5c,

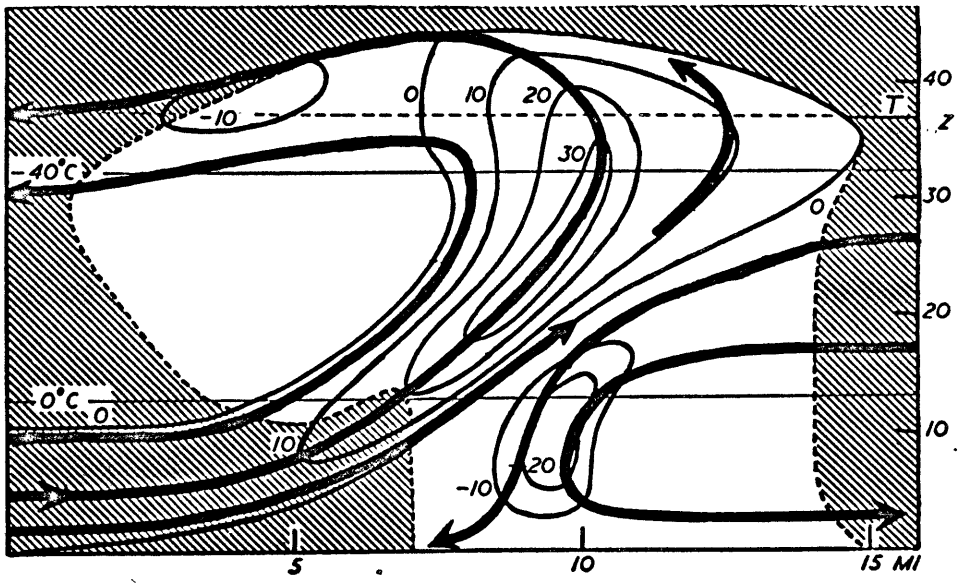

Fig. 5a

Model of a severe thunderstorm proposed by Browning and Ludlam (1960). Streamlines of vertical velocity labelled in m/sec. Unshaded area detectable by radar.

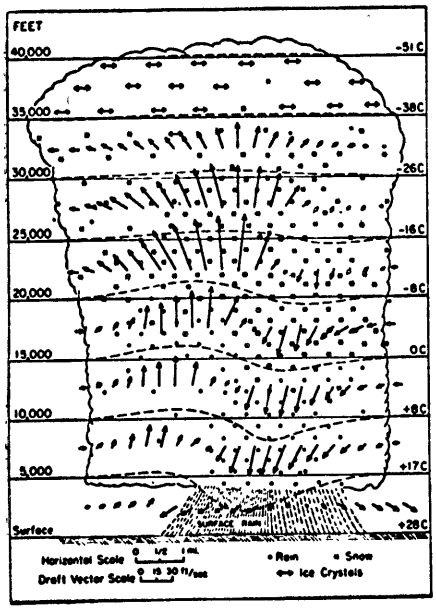

Fig. 5b

Mature stage

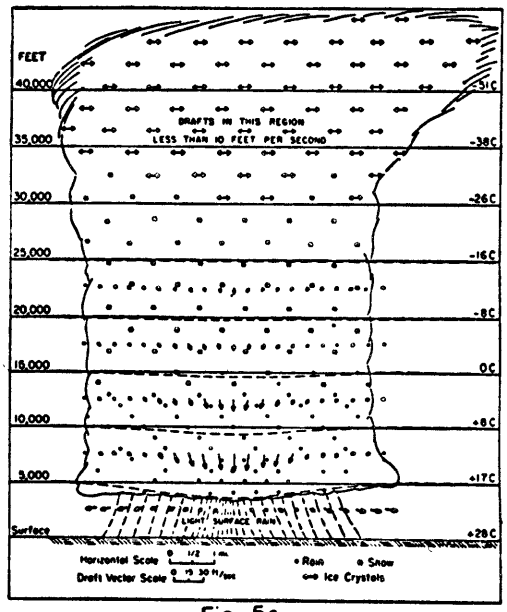

Fig. 5c

Dissipating stage

Single cell thunderstorm model of Byers and Braham (1949)

which is characterized by diminishing upward motions. Ultimately all updrafts cease and only gentle downdrafts remain. Byers and Braham stress that this model is highly idealized and large deviations can be expected for any particular storm or cell. The basic model of the "Thunderstorm Project" has rightly gained wide acceptance throughout the field of meteorology. In recent years more sophisticated radar sets and recording equipment have increased the detail and quality of the basic data; consequently, many investigators have attempted to refine portions of the simple thunderstorm model.

Browning and Ludlam (1960) in their rather detailed analysis of a severe thunderstorm in England present a simple model of the vertical motion field in a mature traveling thunderstorm, see fig. 5a. The unique feature of their model is a tilted updraft which is not impeded by the falling precipitation it generates. Also, moist unstable air can be drawn in from some distance away from the storm or from a region above a stable surface layer. In either case the storm's source of energy is not severed. In short, this type of thunderstorm can maintain a quasi-steady state condition for extended periods of time. Another appealing feature of this model is that the tilted updraft provides a mechanism for recirculating hailstones so that they can attain sizes comparable to those actually observed.

The simple models discussed above suggest certain general characteristics

which should be observable by radar. Normally the cumulus stage is not detected by radar since the number and size of the water drops result in a reflectivity value which is too small for the radar to sense. The initial radar detection should occur about the time the storm first begins to precipitate.

Radars are capable of detecting smaller scale variations in the vertical motion field than are suggested by the simple models previously discussed. RHI photographs taken at low gain settings display many small scale echoes within a larger storm which leads us to infer the existence of convective cells of this general size. Such an inference is substantiated by observations of vertical velocities within thunderstorms made by American Airlines (1949). Their measurements show the existence of many small cells with a lateral dimension of about 1000 ft. Heavy precipitation areas contained as many as 4 of these small cells per mile.

One must be quite careful in drawing conclusions or physical inferences from radar data, particularly RHI data. It is impossible to determine from radar data alone whether an echo or portion of an echo is in a field of positive or negative vertical motion. There seems to be a tendency to associate the strongest portion of the echo with the area of maximum updraft. This need not be the case for the strongest echo region could just as well be linked to areas of strong downward motions. As yet no fully successful scheme has been devised to portray detailed three-

dimensional radar data. Only when such a system is in operation will it be possible to clearly trace the internal development of thunderstorms by radar.

In the following sections particular vertical characteristics of thunderstorms which are observable by radar are discussed and, when possible, linked to one or both of these simple models.

B. Data Reduction

The film record of contour data is continuous throughout periods of storminess and thus provides a basis for identifying time variations of echoes and their eventual dissipation. Contour scans are normally restricted to low elevation angles and therefore are insensitive to vertical variations of reflectivity. Sets of RHI photographs are used to provide vertical cross sections of the storms. By combining the two types of data it is possible to analyze, to some extent, vertical, horizontal and time variations of convective storms.

For days on which widespread convective activity was observed selected contour levels (levels 2, 5, 8 and max.) were traced from the 35 mm film to data sheets on which the 35 mm PPI image is enlarged to a circle 9 inches in diameter. Data sheets were prepared at about 10 minute intervals so that formation, motion and decay of echoes could be determined with ease.

The next step was to relate each series of RHI photographs to the appropriate data sheet and plot the azimuth at which the pictures were taken. After all the RHI photographs for the day had been related to the data sheets it was a simple matter to follow the history of a particular echo or thunderstorm in time and space and to get some idea of its vertical structure. Since this investigation is limited to studying vertical features of convective storms those storm tracks which have few or no RHI photographs associated with them are not considered.

C. Qualitative Analysis

Each storm is studied separately, hence the analysis sheet is arranged so that RHI and contour data follow in chronological order . The first block in each line contains the identifying data for that set of RHI pictures. Items included are the time of the RHI photograph(s) and nearest contour tracing; range, azimuth and pulse setting of the radar; echo width and range as shown by the RHI; and highest contour level observed. When there was a long time gap between RHI sets data from the contour tracings were entered to add as much continuity as possible. The remainder of each line was devoted to the qualitative vertical features to be studied. The features studied are listed below along with a short explanation of why they were selected and the type of result expected.

Maximum Height: This is defined as the highest altitude of the echo being studied as observed on the most sensitive gain setting of the AN/CPS-9 (usually gain 10). At close ranges, less than 25 miles, the most sensitive gain setting used was normally gain 8 or 6. No loss of sensitivity resulted because the minimum detectible reflectivity of gain 10 on long pulse at 1000 miles is about the same as that of gain 8 on short pulse at 25 miles.

Byers and Braham's model suggests that a single celled thunderstorm should have a single maximum height during its lifetime and it should be reached early in the mature stage. On the other hand, a multi-celled storm might have a number of maxima corresponding to the maturity of one or more of its interior cells. Data collected in this section are to be used to study the variation of echo tops with time and as a function of the intensity of the storm.

Appearance of Edges and Top: In this section entries are limited to remarks such as sharp, blurred, fuzzy, or chaotic and are restricted to RHI pictures taken at gain settings 10 or 8. Statements such as these are intended to give a general idea of the gradient of reflectivity at the edge and top of a storm. A very sharp outline is interpreted as indicating the edge of a strong discontinuity in vertical motions such as would be expected at the edge of a young or rapidly intensifying cells. A blurred or fuzzy outline implies weak vertical motions or a predominance

of snow as a reflector. It can be expected that a fuzzy top indicates glaciation and would be noticed before the appearance of an anvil top or cap cloud.

Vertical Description: This category is used to describe the main features of the vertical structure of the storm such as discernible turrent, uniformity or variations in width, taper, or bulges. One would expect the storm's vertical structure to vary considerably during its existence, also variations can be expected across the lateral dimension. The persistence and extent of these features may be helpful in determining a future state of the storm. Variations of this type have been smoothed out in the simple models, presented earlier. At close ranges the resolution of the radar beam increases, consequently, many irregularities appear on the RHI pictures. When the irregularities are too complex to describe the picture is termed "chaotic".

Tilt: A simple yes or no and the basic direction of the tilt is recorded here. The results should be dependent upon the angle between the mean upper level wind direction and azimuth of the RHI observations. According to Byers and Braham vertical transport and mixing of momentum caused by the initial strong updrafts and entrainment result in nearly vertical radar echoes. As vertical motions in the storm subside mixing of momentum decreases and tilting should ensue. The degree of tilt will depend upon the strength of the vertical wind shear. In direct contrast, the model

proposed by Browning and Ludlam suggests that the tilt would be into the prevailing wind because of the tilted vertical motions. Also, the greatest tilt should be observed when the storm is most intense.

Contraction of the horizontal scale of the RHI at 50 and 100 mile ranges makes it difficult to observe small tilts. Also, sufficient upper wind observations were not available to permit detailed study of the wind fields around the storms and, consequently, the variation of tilt with time.

Anvil or Cap Clouds: Here, too, only yes and no entries are necessary. Since anvil or cap clouds normally consist of snow or ice crystals they can be detected only on the most sensitive gain settings, normally gains 10 or 8. Formation of an anvil is associated with the mature and dissipating stages of the model suggested by Byers and Braham. They may also be a function of the maximum height of the storm, or better, the temperature at that level. If the occurrence of an anvil or cap cloud can be linked to the dissipating stage of a thunderstorm then its appearance would be a useful forecasting tool.

Number of Internal Cells: At reduced gain settings only the most intense precipitating echoes are observed. The number of these cells is thought to be connected with the size and severity of the storm. Again the radar's ability to observe and display these small scale features is highly dependent upon the range of the storm and range setting of the RHI.

Increase of Reflectivity with Height: Donaldson (1958, 1960) prepared reflectivity profiles of severe thunderstorms from 3-cm band radar data. The profiles were constructed from many series of PPI photographs taken at numerous gain steps and elevation angles. From these profiles Donaldson concludes that severe thunderstorms are characterized by higher reflectivity values aloft (20-30,000 ft) than at the surface. He contends that the storage of large amounts of hail by the strong updrafts at these high levels results in a substantial increase in radar reflectivity. This section is included as an independent check of his findings. Each series of RHI photographs is examined to see if strong precipitating storms show any evidence of high reflectivity cores at these altitudes.

Remarks: This section is inserted so that pertinent statements not applicable to other categories may be included. A particularly important remark is one giving the relation of the RHI azimuth to the most intense portion of the cell, such as center cut, off center cut, edge cut, etc.

D. Synoptic Background

Severity, size, and duration of middle latitude thunderstorms seem to be intimately linked to the current synoptic pattern. Generally, the most severe and long lasting storms are associated with cold frontal squall lines, while those designated as "air mass thunderstorms" are shorter lived and less severe. This concept is confirmed by the storms

of 30 June and 10 July 1961. A brief description of the synoptic situation and upper air patterns for these two days is given as a basis for studying the differences and similarities of storm features.

The storms of 30 June were the result of a weak cold frontal squall line and solar heating. The cold front had a NE-SW orientation and moved through New England during the afternoon and early evening. A weak upper level trough was associated with the front and gave rise to WSW winds ahead of the front and west to westnorthwest winds after frontal passage. An upper air sounding taken at M.I.T. shortly before the squall line passed showed that the wind direction above 5,000 ft was nearly constant at 290 degrees. The wind velocity increased from 25 knots at 10,000 ft to 55 knots at the tropopause level of 38,000 ft. Radar echoes began to form shortly before noon over central and northern Massachusetts. In fig. 6 the tracks of the major storms are shown. The tracks labelled storms 1, 2, 3, 5 are the only ones included in the study. Storm 1 was the longest and most severe of the day. Storm 3 formed behind and to the west of storm 1 and followed roughly the same path. It too was a very intense storm. Storms 2 and 5 were not as intense as 1 and 3 and dissipated rapidly once they moved over water. There was a surprising lack of smaller storms in between the larger ones.

On 10 July there were no discernible fronts in New England. The convective activity was associated with a weak upper level trough which

drifted over New England during the day and the usual afternoon solar heating. Convective echoes began to form about noon with rather random positioning and during the afternoon and early evening more than 40 separate storms occurred. The storms were small, short lived and only moderately intense. No radiosonde observation was taken at M.I.T. but analysis of data from surrounding stations showed the winds to be from the west at 20 knots below 15,000 ft and backing to southwest at 30 knots near the tropopause level of 30,000 ft. The tropopause was very sharp which accounts for the fact that only two storm tops were observed above 30,000 ft. The storms moved slowly and somewhat erratically toward the east and northeast.

E. Results of Qualitative Analysis

This section is devoted to results of analyzing the vertical features discussed earlier. In some cases only very broad statements can be made, while for others interesting results can be discussed in more detail. Figures 7, 8 and 9 at the end of this section contain selected RHI photographs which illustrate some of the more important features. Fig. 7, for instance, contains three series of RHI pictures taken of the same storm, storm 1 of fig. 6, over a period of 16 minutes and illustrates the formation of an anvil top, complex interior structure and rapid variation of internal features.

Maximum Heights: The height of the echoes at the time of initial detection varied greatly. The times of initial detection for the two radars are not the same. A cell should be observed first on the more sensitive AN/CPS-9; however, due to the manual method of operation it was not always possible to take RHI pictures within a few minutes of an echo's first appearance. In all cases for which RHI pictures were taken both before and after initial detection by contours the latter height was highest. Fig. 8a illustrates the initial growth of storm 1 of fig. 6. For the first 30 minutes the storm developed slowly then intensified rapidly. Slow initial growth was not typical of the storms of 30 June. Storm 2 of fig. 6 was detected first on contours at level 2 (R of 2 mm/hr), 12 minutes later it had intensified to level 8 (R of 150 mm/hr) and a RHI observation at this time showed a top of 34,000 ft, which, incidentally was the maximum height attained by this storm.

Storms of 10 July did not grow and intensify as rapidly as those just described. One echo had attained a height of 12,000 ft 9 minutes prior to the initial contour observation and an hour later its top was only 26,000 ft. Generally speaking the storms on both days grew to about 75% of their maximum heights within 20-30 minutes after initial detection by the SCR-615-B.

Variation of echo tops throughout the life of the storm is difficult to analyze. A large number of RHI observations, more than were available

for this study, are needed to adequately cover the spatial and temporal changes. Data available seem to indicate that variation of echo height across the storms, particularly large storms, is greater than changes observed over short periods of 10-20 minutes. The storms of 10 July reached only one maximum both in height and intensity and then dissipated slowly, thus supporting, to some extent, Byers and Braham's single celled model. On 30 July the storms reached their maximum heights quickly and then undulated by as much as 10,000 ft for the remainder of their active stages. This behavior is characteristic of a multi-celled storm. On neither day were the times of maximum height and of maximum surface intensity consistently related.

Appearance of Edges and Tops: Results obtained from this section were disappointing. The sharpness of storm features seemed to be closely related to variations in photographic processing, intensity setting of the RHI, and range at which the storm was observed. Overexposure of the photographic film or paper tends to blur the edges of the storm and eliminate much of the small-scale interior detail. Pictures of large storms at 10 and 25 mile ranges displayed more detail than can be treated in this study. In spite of these handicaps some useful relations were obtained.

In nearly every case edges of young storms were clearcut and free of bulges or other major discontinuities, see fig. 8a. In the mature stage

the clarity of the edges varied considerably. The storm portrayed in fig. 7 is a good example. At gain 10 the rear edge is fairly well defined in all three pictures, however, the front edge is ragged and discontinuous (7a) and undulating in 7b and 7c. The sides and top of the storms shown in figs. 9d and 9e also display a very jagged appearance. As storms began to dissipate all the features take on a fuzzy or blurred character, see figs. 8b, 8e, and 9c for example. An attempt to link occurrence of anvil or cap clouds with previous observations of blurred or fuzzy tops failed. In fact in one case RHI observations one minute apart in different portions of the same storm showed a sharply defined top at one point and well formed anvil at the other.

Vertical Description and Interior Cells: In the early stages of formation and growth most convective storms displayed nearly vertical sides and uniform widths, particularly in lower levels (0-20,000 ft), with turrets or spires extending another 10-20,000 ft higher. As the storms intensified the wider portion extended to greater heights until the turrets disappeared or remained as slight undulations in the top. Fig. 8a exhibits such a case. Only for the two large storms of 30 June, storms 1 and 3 of fig. 6, were sufficient RHI observations available to study some of the variations of vertical features in detail. Storm 1 passed extremely close to the radar and at such close ranges so much detail is displayed that it is difficult to select the really important features. The photographs of

figs. 4, 7, 9d, 9e show how complex and detailed the interior of storms can be.

During the mature stage the external and internal structure of the storms varied greatly. One more prevalent feature observed was an indentation or constriction of one or both edges near the melting level. Examples of such behavior are best shown by figs. 7c, 8e (both cells), 9a, 9b, 9e. In some cases the bulge above the melting level is found to consist of small cells adjacent to the main core very much like those seen in fig. 7c at gain settings 8 and 6. A possible explanation is that the smaller cells are at the edge of a rising current which contains many small water droplets. A certain amount of entrainment is occurring at all levels and above the melting level large quantities of snow or ice crystals can enter the updraft from the relatively quiescent region near its edge. As the mixture of ice and water droplets travels upward water diffuses onto the ice surfaces. Physically it is possible for the diffusion to take place so rapidly that the latent heat released is sufficient to keep the ice surfaces wet. In this condition the particle will take on the reflectivity properties of a liquid water drop of the same size and shape, thereby increasing the observed radar reflectivity, similar to the "bright band" effect in reverse.

The number of interior cells observed at low gain settings tended to be inversely related to the storm's intensity at that time. This is

reasonable in that during the intense stage vertical motions are well organized and RHI photographs would be expected to show a small number, 1 to 3, of large intense echoes. As the strong vertical motions diminish smaller eddies form and impart a somewhat chaotic nature to subsequent RHI observations. Fig. 7c is a prime example of a well organized intense storm while figs. 7a and 9d display a confusion of interior cells.

Anvil or Cap Clouds: Surprisingly, anvil or cap clouds appeared on relatively few RHI photographs. On 10 July only 3 of the 9 storms studied had anvils during some portion of their lives. Storms 1 and 3 of 30 June were an hour and a half old before any anvil type clouds were observed by radar and not all succeeding photographs showed anvils. As mentioned earlier nearly simultaneous observations over different portions of one storm showed that the anvil can exist in one region and not in another. Again storm 1 of 30 June serves as the best example. The gain 10 pictures of fig. 7 show the initial evolution of the anvil top. At this point the storm is an hour and 40 minutes old. The pictures of fig. 9e were taken about an hour later and suggest the presence of cirrus but not a well defined anvil, and the photographs of fig. 4 taken later yet show no hint of any anvil. As the storm moved southeastward an anvil appeared again for a short time but during the last hour of its life no anvils were observed by the radar.

A classical example of a dissipated storm is shown in fig. 9c. At

gain 10 the front cell gives the appearance of being fairly strong, but only a little fuzz remains at gain 8 (R less than 1 mm/hr). Within a few minutes this cell disappeared from both radars.

The only conclusion which can be drawn from this section is that radar observations of the presence or absence of an anvil are not correlated with a distinct stage of a storm's existence, particularly the dissipating stage. In fact, if the model proposed by Browning and Ludlam is correct one would expect the anvil to form during the most intense stage because of the large amount of moisture carried upward and ahead of the storm.

Tilt: On 10 July the wind shear was very slight and only one storm exhibited any noticeable tilt. On 30 June wind shear of 30 knots between 10 and 35 thousand feet produced some interesting effects. Each of the four storms of this day are discussed separately.

Storm 1 began to the northwest of M.I.T. and for 2-1/2 hours the RHI sections were nearly parallel to the upper level winds. No noticeable tilt was evident until it had passed its first intensity maximum about two hours later. An RHI series at this time showed a well defined tilt to the northwest (top further to the NW than the base), or opposed to the prevailing wind shear. The cell which exhibited the reverse tilt was on the southwestern edge of the storm complex. A close study of the contour data indicated that this was a new cell, a contention which is

further supported by a southward dip of the storm track at about the same time. A few minutes after the RHI pictures were taken the new cell was the most intense in the storm. The reverse tilt evidently resulted from the initial vertical motion field of the new cell. A few minutes later the tilt had vanished. Later, when the storm was a few miles southwest of the radar site, a pronounced cross wind tilt (top tilted toward the NE) was noted for two small cells which were dissipating at the rear edge of the main storm (see fig. 8d). No immediate explanation for this effect is evident. The storm continued to move to the southeast and during the last hour of its life the top tilted slightly toward that direction.

Storm 2 also began in the northwest quadrant and the first RHI photographs showed a definite tilt of the top toward the northwest, again opposed to the prevailing shear. In a short time the tilt disappeared. During its most active stage the storm was situated to the north and east of M.I.T. so that the RHI observations were taken at nearly right angles to the upper level winds. As the storm moved eastward over the water and began to dissipate a slight tilt toward the east (inner echo of fig. 8e) was observed.

Storm 3 developed in the southwestern quadrant and moved to the southeast hence for the first hour or so the RHI observations were taken in a cross wind sense and no tilting was noted. For the remaining two

hours a slight tilt of the top toward the southeast was detected (see fig. 8b).

Storm 5 sprang up east of Cambridge with a pronounced eastward tilt. It straightened up during its short mature stage and then succumbed to a slight eastward tilt again as it dissipated (see fig. 8c).

The reverse tilts observed for storms 1 and 2 were directly connected to new cell development indicating that the initial vertical motions were canted in this direction and vigorous enough to override the environmental wind shear. Thus it can be reasoned that during their mature stage the internal forces and vertical motions of intense thunderstorms can neutralize the ambient shear and even produce shear in the opposite sense. The vertical motion field shown in the model storm suggested by Browning and Ludlam is very similar to that just described. Dissipating thunderstorms exhibit a definite preference for tilts in the direction of the prevailing atmospheric shear.

Increase of Reflectivity with Height: Storms studied in connection with this category were not limited to 30 June and 10 July but included all RHI photographs of thunderstorms taken during the spring and summer of 1961 (May to September). Each series of RHI pictures was examined for any evidence of elevated reflectivity cores. To qualify as a positive occurrence the storm was required to be precipitating at the surface, discernible at gain 4, and the base of the high reflectivity core must

not extend below 10,000 ft. In all fairness it must be emphasized that the observational technique followed in gathering the data is very dissimilar to Donaldson's method. However, if his assertion is correct and high reflectivity cores are characteristic of severe thunderstorms then these arbitrary restrictions will have little effect on the outcome of the analysis.

Of more than 150 RHI series on which echoes were discernible at gain 4 only 10 occurrences of elevated reflectivity cores were found. In all 10 cases the base of the core was between 10 and 20 thousand feet and at no time did their tops reach above 30,000 ft. The storm shown in fig. 8d at about 15 miles range is one of the positive cases. A large majority of the 150 RHI series were of hail producing storms including storm 1 of 30 June which produced a hail track 100 miles long and 10-20 miles wide (Geotis, 1961). Contrary to Donaldson's hypothesis these storms routinely displayed the region of maximum reflectivity reaching the ground. Numerous examples are shown in the figures, the most striking being the gain 4 picture of fig. 7c which shows the intense core reaching from the surface to 30,000 ft. Figs. 9d and 9e are also fine examples.

A strict comparison of these results with Donaldson's findings is not possible since the RHI data are not sufficiently accurate, but they do demonstrate that elevated reflectivity cores are not frequently observed on the RHI. The basic data for both studies originated from the same model

radar, AN/CPS-9, yet conflicting results ensued. It is likely that the differences are a result of observational technique and method of analysis rather than the capability of the radars.

In connection with Donaldson's work the effects of attenuation may be considered in more detail than he found possible. He concludes his subjective discussion of attenuation by saying, "The problem of attenuation distortion will never be settled satisfactorily, however, until a measurement of rain intensity through the core of a thunderstorm is obtained coincident with reflectivity profile observations", (Donaldson, 1960, page 123). Section III of this paper is the first step in this direction. Reflectivity measurements obtained from a 3-cm band radar are compared with coincident measurements from a 10-cm band radar. Since the 10-cm radar measurements suffer little attenuation they are indeed an independent measure of actual reflectivity values. The decrease in reflectivity suffered by the 3-cm band radar when viewing an intense thunderstorm is successfully explained by considering the effects of attenuation. Further, it is shown that attenuation cannot be neglected at 3-cm wave lengths particularly when dealing with quantitative measurements of reflectivity in regions of moderate to heavy rain.

The effect of attenuation on observed radar echoes is twofold. Distortion, such as shown in fig. 2, leads one to the false impression that the most intense portion of the storm is on the side nearest the

radar. The amount of distortion is directly proportional to the storm's intensity. Since the bulk of the thunderstorms observed in New England move in from the west distortion such as this would lead Donaldson to his fallacious conclusion "Typically, the rain intensity in a thunderstorm increases sharply from the forward edge, with a maximum near the forward edge and a relatively long, gradual decrease toward the trailing edge." (Donaldson, 1960, page 123). In direct contrast, Geotis, 1961, finds from 10-cm band radar data that the most intense precipitation is usually found near the storm's center. The type of distortion illustrated by fig. 4 is even more damaging. In this situation the area of heavy rain between the radar site and the most intense cell of the storm complex caused the 3-cm band radar to pick the wrong cell as "most intense".

The foregoing remarks do not refute the possible existence of reflectivity cores aloft, but are intended to show that differing conclusions may be drawn from data taken from the same model radar and that Donaldson's findings are based on an incomplete analysis of the possible causes. Until more reliable data are obtained, namely from 10-cm band radar, one is forced to view with skepticism the correlation of elevated reflectivity cores, as observed by 3-cm band radar, with severe thunderstorms and any forecasting scheme based on such a premise.

V. CONCLUSION

The effects of attenuation by rain at 3-cm wave lengths have been reviewed and applied to observed cases. The results indicated that:

1) Attenuation caused by heavy rain cannot be neglected for quantitative radar measurements. Obviously, the reflectivity values observed under such conditions are greatly underestimated. Losses caused by attenuation cannot be satisfactorily recovered.

2) 3-cm radars display a poor picture of the relative intensity of cells within a severe thunderstorm. As fig. 4 shows it is possible for the radar to select the wrong cell within a echo complex as "most intense".

3) Distortion caused by attenuation produces an apparent displacement of the storm's core toward the radar (see fig. 2) and the degree of distortion increases as the storm intensifies.

The thunderstorms studied are characterized by an initial period, 20-30 minutes, of rapid growth and intensification. The mature stage varied in duration from several minutes to several hours and exhibited complex and variable internal and external features. Fluctuations of the vertical features bear no simple relationship to a stage in the storm's life history and hence one cannot deduce from them how much longer the

storm may last or what its future intensity will be. The storms dissipated about as rapidly as they formed. RHI photographs of dying storms displayed a nearly uniform area of reflectivity such as that shown by the inner storm of fig. 9c.

The more important conclusions and inferences obtained from studying the vertical features of thunderstorms are:

1) That the number of internal cells observed at low gain settings tends to be inversely proportional to the current intensity of the storm. This relationship leads one to believe that during its intensity maximum the field of vertical motion is well organized and relatively free of small scale eddies.

2) That anvil tops can be observed continuously or intermittently during the mature and dissipating stages. The presence of an anvil is no indication that the storm is or will be dissipating within the near future.

3) That dissipating storms tend to tilt in the direction of the prevailing wind shear. In contrast, some mature thunderstorms displayed tilts which were not caused by synoptic scale wind shear. The appearance of tilts opposed to the prevailing wind shear were linked to the initial period of growth of the cells involved and indicate that the field of vertical motions was canted into the wind.

4) That in intense thunderstorms elevated reflectivity cores are

seldom observed on the RHI. Further, it is shown that the effects of attenuation are such that observations of increased reflectivity cores by 3-cm radars are virtually meaningless.

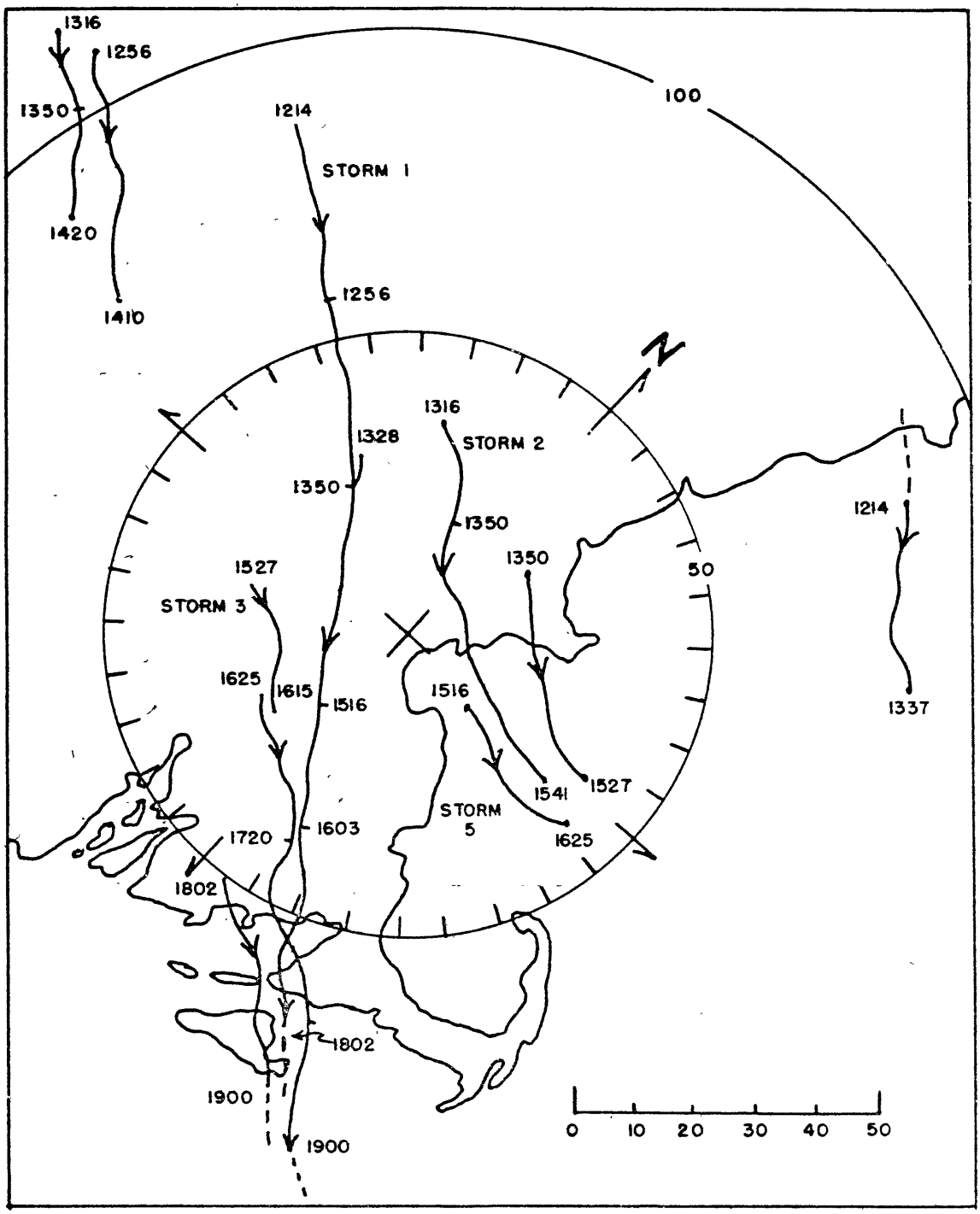

Fig. 6. Paths of the major storms of 30 June 1961

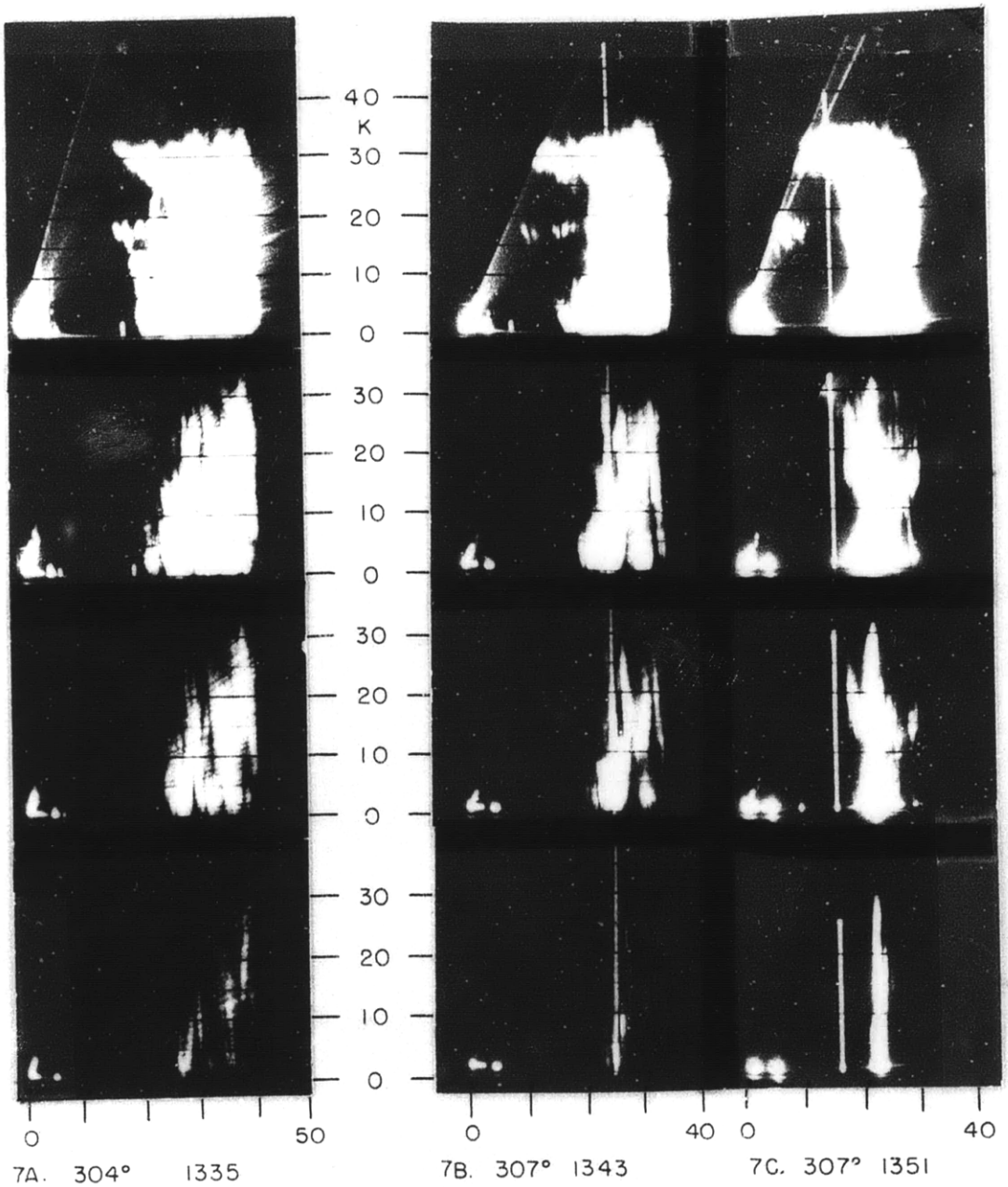

Fig. 7. RHI photographs of storm I (fig. 6). Gain settings are 10 (top), 8, 6, 4 (bottom) on short pulse. The strong core of 7C is faintly visible at G-2 (not shown).

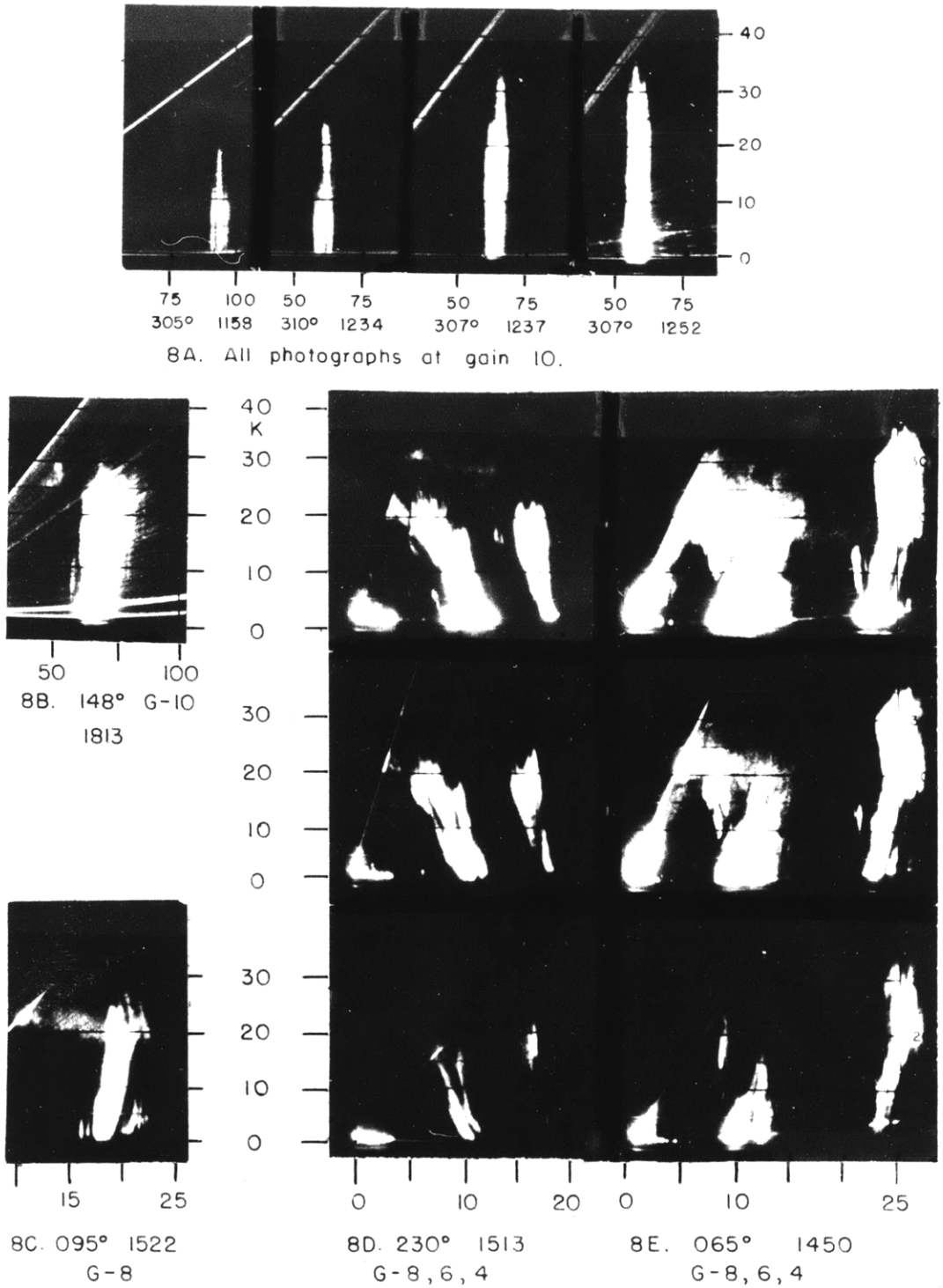

Fig. 8. Selected RHI photographs for storms of 30 June 1961.

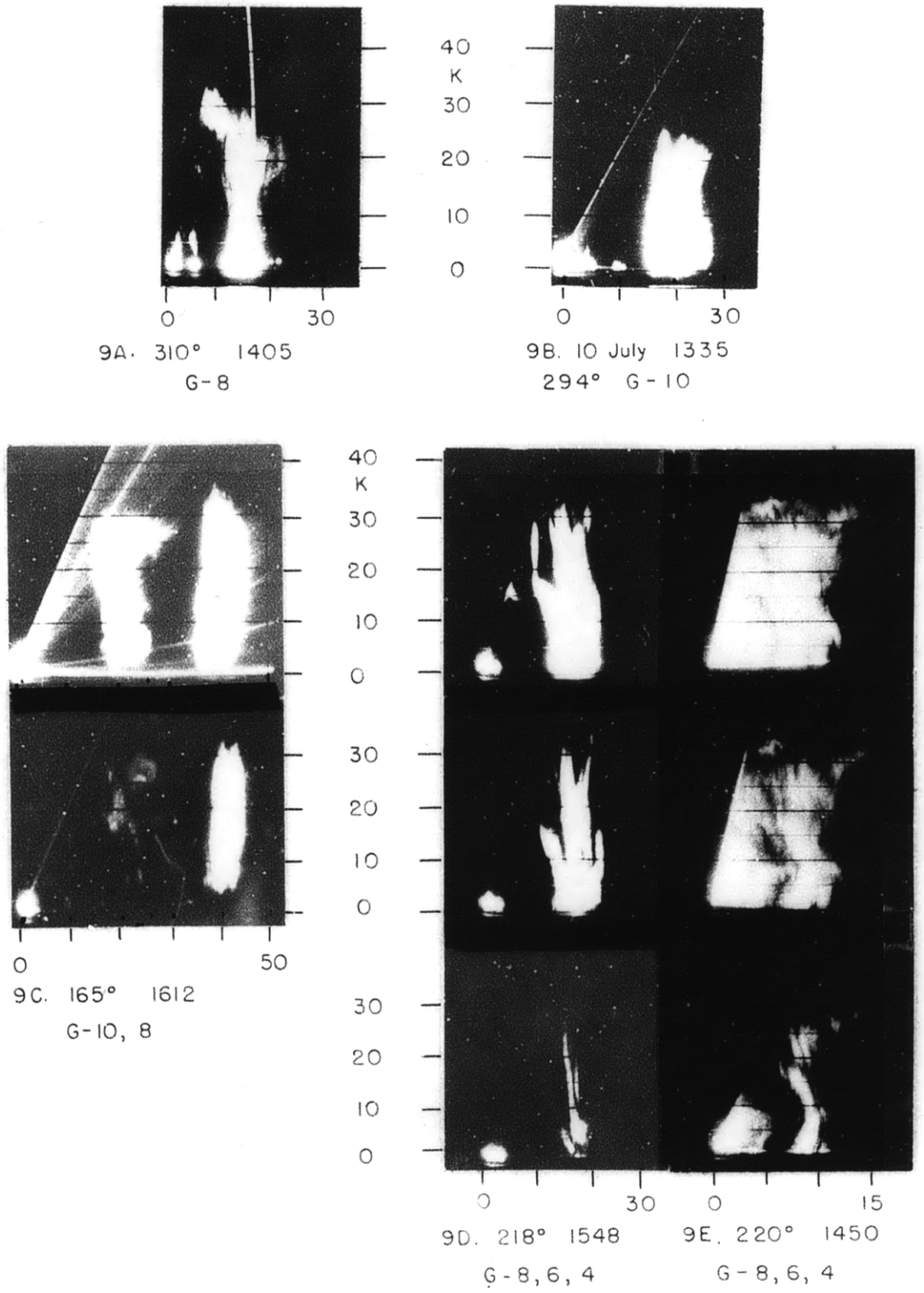

Fig. 9. Selected RHI photographs for storms of 30 June 1961 — except 9B.

REFERENCES

American Airlines System, 1949: The Development of an Airborne Radar Method of Avoiding Severe Turbulence and Heavy Precipitation Areas of Thunderstorms and Squall Lines. Final Report on Task No. 1, Navy BuAer Contract NOa(s)-9006.

Austin, P. M., 1961: Some Observations of Attenuation of 3.2 cm Radiation by Heavy Rain. Proceedings of the Ninth Weather Radar Conference, American Meteorological Society, Boston, Mass., pp 325-330.

Austin, P. M., and S. P. Geotis, 1960: The Radar Equation Parameters, Proceedings of the Eighth Weather Radar Conference, American Meteorological Society, Boston, Mass., pp 15-22.

Battan, L. J., 1959: Radar Meteorology, Univ. of Chicago Press, Chapt. 11.

Byers, H. R., and R. R. Braham, 1949: The Thunderstorm, U. S. Gov't. Printing Office.

Donaldson, R. J., Jr., 1958: Analyses of Severe Convective Storms Observed by Radar, Journal of Meteorology, 15, pp 44-50.

Donaldson, R. J., Jr., 1960: Thunderstorm Reflectivity Structures, Proceedings of the Eighth Weather Radar Conference, American Meteorological Society, Boston, Mass., pp 115-125.

Geotis, S. P., 1961: Some Radar Measurements of Hail, Proceedings of the Ninth Weather Radar Conference, American Meteorological Society, Boston, Mass., pp 133-318.

Gunn, K. L. S., and T. W. R. East, 1954: The microwave properties of precipitation particles, Quarterly Journal of the Royal Meteorology Society, 80, pp 522-545.

Kodaira, N., 1959: Quantitative Mapping of Weather Radar Echoes, Research Report No. 30, Weather Radar Research, M.I.T., Cambridge, Mass.

Ryde, J. W., and D. Ryde, 1945: Attenuation of Centimetre and Millimetre Wave Lengths by Rain, Hail, Fogs and Clouds, Report No. 8670, Research Laboratories of the General Electric Co. Ltd., Wembley, England.

Wein, M., 1961: The Electronic Correction for Attenuation of 3.2 cm Radar Signals from Rain, Proceedings of the Ninth Weather Radar Conference, American Meteorological Society, Boston Massachusetts, pp 367-370.